Tornado Vortex Simulation at Purdue University

C. R. Church, J. T. Snow, and E. M. Agee

Department of Geosciences
Purdue University
West Lafayette, Ind. 47907

Abstract

A 4 m wide and 7 m tall tornado vortex generator (including exhaust fan and duct work) has been constructed at Purdue University that operates on a principle similar to that of the earlier machine modeled by Ward (1972). Characteristics of the Purdue simulator are described, as well as the corresponding modifications and improvements that have been made to Ward's machine. Selected photographs of vortex configurations obtained in the simulator demonstrate the ability of the machine to achieve vortex breakdown and multiple vortex configuration. A radial-axial profile of velocity magnitudes (using hot-film anemometry) has been obtained for the state of vortex breakdown characterized by two interlocking helical spiral vortices. This preliminary result shows the potential that the experimental system offers for obtaining quantitative information about the flow field of selected vortex configurations. Multiple vortex phenomena in the thunderstorm-tornado system are examined in light of the laboratory simulation and the similarity concept.

1. Introduction

Research in the Department of Geosciences at Purdue University is focusing on the laboratory simulation and study of tornadolike vortex features, with primary emphasis on a *quantitative* investigation into the nature and cause of the multiple vortex phenomenon. Efforts thus far have resulted in the construction and successful operation of a "tornado" vortex generator designed after the machine developed by Ward (1972). The characteristics of this simulator and the corresponding modifications and improvements that have been made to Ward's original machine are discussed below. Even though the initial effort in the research thus far has been devoted primarily to the design, construction, and successful implementation of the experimental system, the experimental phase of the research has begun and preliminary results will also be discussed in this paper.

The systematic collection of pertinent and relevant physical data within and near a real tornado vortex is precluded by the sporadic occurrence and extreme violence associated with such an event. Consequently, laboratory modeling offers a viable alternative for obtaining information about this phenomenon. Correspondingly, a rather general body of knowledge pertaining to observed tornado features and behavior that lend themselves to laboratory study has begun to accumulate over the years from the earlier observations by Van Tassel (1955), Fujita (1959), and Hoecker (1960) to more recent observational findings, e.g., Agee *et al.* (1975, 1976, 1977). Such study affords the researcher an opportunity to control the conditions of the vortex environment and thus allows for the identification and investigation of those parameters that govern various types of vortex formation and behavior with time.

Some pertinent observational findings in the study of tornado damage tracks, photographs, and movies of tornadoes, as well as eyewitness accounts, are now discussed. Van Tassel's (1955) early recognition of a cycloidal debris pattern in the North Platte, Nebr., tornado gave a new dimension to the analysis and interpretation of debris patterns subsequent to that time. Later, Fujita's (1971) observation of a dust devil system in central Illinois confirmed the presence of multiple vortices that were moving clockwise around a common center, and this coupled with additional observations of cycloidal debris patterns in tornado tracks led to Fujita's concept of suction vortices within a tornado system. Photogrammetric documentation of the multiple vortex phenomenon in a parent tornado system, including the *life cycle* of individual suction vortices, was presented by Agee *et al.* (1975). Subsequent work by Agee *et al.* (1976, 1977) has revealed that the multiple vortex phenomenon persists at several scales of motion within the thunderstorm-tornado cyclone event. A study by Georges (1976) suggests that acoustic waves radiating from multiple vortex systems can be detected, and his theoretical calculations are consistent with the observational reports by Agee *et al.* (1975, 1976). In fact, the hierarchy of multiple vortex systems reported by Agee *et al.* (1976) may be even more complex than realized. This is supported by the study of the West Lafayette, Ind., tornado system of 20 March 1976 (Agee *et al.*, 1977) and also by unpublished findings in a current study of the central Iowa tornado family of 13 June 1976.

The hierarchy of multiple vortex phenomena based on all available knowledge is now revised as shown in Fig. 1. The split of the so-called mini-tornado cyclone α into the mini-tornado cyclones β represents still another intermediate scale of multiple vortex behavior prior to the actual tornado, which is suggested in the analysis of the tornado damage tracks of the Iowa tornado family. The amount of observational data now accumulating points to the significance and importance of studying the multiple vortex phenomenon and developing a complete stability theory based on both experimental and theoretical considerations that offers a full understanding of the fluid mechanics of this problem as well as an understanding of its application to the interpretation of atmospheric events. Agee *et al.* (1976) have already shown how critical the recognition and treatment of this feature in tornadic thunderstorms are to proper tornado warning. A specific example to il-

lustrate this point can be taken from the 3 April 1974 outbreak. A family at a farmstead near West Lafayette, Ind., was watching a tornado move to the north of their location when a second tornado in a parallel mode event struck their location. A similar event happened to Charles Barthold of WHO-TV, Des Moines, Iowa, when he was filming the Iowa tornado family on 13 June 1976.

Even though the multiple vortex phenomenon is one of the more interesting dynamic features that has been realized in tornado-thunderstorm systems, other observational features also merit consideration. Once a tornado cyclone has formed, it becomes necessary that the flow field concentrate ambient vorticity in the process of producing a tornado. Agee *et al.* (1977) have discussed this from the standpoint of the observation of both a rotating tail cloud and the occurrence of concentrated bands of damage along a spiral path associated with the inflow into the region of the tornado. Since Fujita's (1959) early observation of the tail cloud in the Fargo tornado and Golden and Purcell's (1975) more recent observation of a dust cloud (or vorticity feeder band) in the Great Bend, Kans., tornado, a clearer conception of the mechanism of vorticity concentration may be emerging. This aspect of a tornado vortex formation lends itself to laboratory simulation and experimental investigation.

Other aspects of laboratory experimentation related to tornado observations can pertain not only to the multiple vortex phenomenon but also to the development of laminar and turbulent vortices and the associated vortex bubble formation that moves down the main core of the vortex system as transition occurs. This will be discussed in more detail in a later section when experimental work in progress is reviewed. It is notable at this point that the development of a strong axial downdraft may be the critical feature that leads to multiple vortex formation, since this feature should result in a strong shear zone in an annulus region that may become unstable to azimuthal perturbations. (It should be pointed out that the axial downdraft may actually be occurring in response to the radial pressure gradient and is more of a response to the development of a strong shear region rather than the cause.) Also it is possible to study vortex geometry and its behavior in time as conditions are varied from weak swirl to strong swirl. This feature is complicated in the atmosphere by the variable amount of water vapor and the degree of availability of surface debris and dust particles.

A quantitative study of vortex breakdown and the occurrence of the multiple vortex phenomenon in an air vortex chamber is the main item of research discussed here, even though a great deal of related information about the dynamics of vortices in general may be ascertained or replicated. A review of the many pertinent and relevant laboratory studies is not presented since it is not the authors' intent to write a review paper. Also, the host of problems associated with laboratory simulation, flow visualization, and measurement techniques are not reviewed as this would require an even greater effort that would perhaps detract from the present objective. However, specific studies and techniques directly related to this experimental effort will be discussed. A review on the laboratory simulation of tornadoes has been presented by Davies-Jones (1976), which should be referred to for details not provided below.

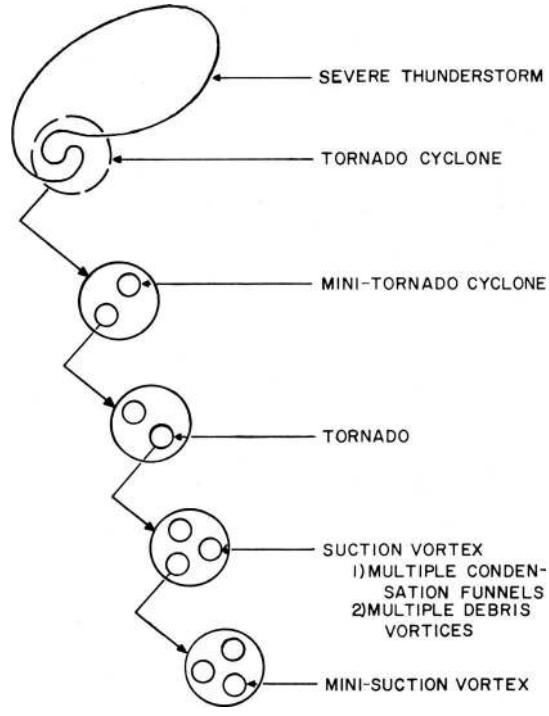

FIG. 1. Hierarchy of multiple vortex phenomena in the thunderstorm-tornado system.

2. Vortex generator and its principle of operation

Up to the present, the principal effort has been directed toward the development of the research facility, the assembly of the vortex generator, and the development of the instrumentation used in conjunction with it. Efforts began in 1975 with a bare room of some 70 m² floor space on the third floor of the Purdue Geosciences Building. This room has now been developed into a vortex modeling laboratory. The focal point of the facility is the vortex generator shown in Fig. 2. The assembled generator measures some 4 m in diameter and 7 m high, including the fan and duct work located on the floor above. As previously stated, the principle of operation is based upon the tornado modeling concepts put forth by Ward (1972) of the National Severe Storms Laboratory. It was our primary goal to produce as stable a vortex as possible so as to facilitate quantitative measurements and to incorporate as many of the recommendations of Jischke and Parang (1974, 1975) as possible following their experience with Ward's apparatus. In the design of the Purdue vortex generator, several

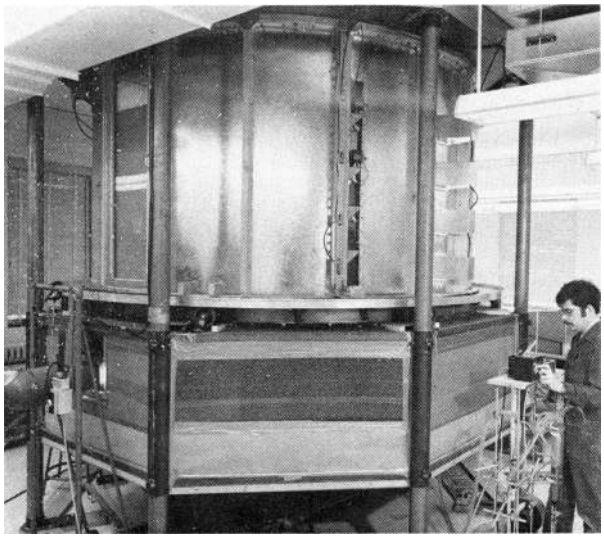

FIG. 2. Tornado vortex simulator at Purdue University.

areas were addressed in which there was room for improvement. These areas are outlined below in the description of the development and operation of the completed machine, where reference is also made to the effectiveness of the improvements.

The basic mode of operation is to cause air to converge toward the center of a cylindrical system, horizontally divided into two chambers. Air converging in the lower chamber is given angular momentum upon passing through a rotating mesh screen. The convergence process then results in the formation of an intense vortex along the central axis of symmetry, as air is extracted from the top of the system. As shown by nondimensionalizing the governing equations of motion (Lewellen, 1962), the type of vortex produced depends strongly on four parameters: 1) radial dimension r^*, 2) axial dimention z^*, 3) circulation Γ^*, and 4) volume flow rate per unit length Q^*. These four parameters can be combined into a single characteristic nondimensional number, the swirl ratio S, defined [1] as

$$S = r^*\Gamma^*/2Q^*z^*, \tag{1}$$

which principally determines the nature of the flow. Application of (1) to the system depicted in Fig. 3 yields the following form for S,

$$S = r_0\Gamma_s/2Q_sh. \tag{2}$$

Since $\Gamma_s = 2\pi r_s V_{\theta_s}$ and $Q_s = 2\pi r_s V_{r_s}$, (2) becomes

$$S = (V_\theta/V_r)_{\text{screen}}/2a, \tag{3}$$

where a is the aspect ratio defined as h/r_0. By applying conservation principles, one can express $r_sV_{\theta_s}$ as $r_0V_\theta(r_0, h)$ and (3) can be rewritten as

$$S = V_\theta(r_0, h)/(\bar{V}_z)_{\text{updraft hole}} \tag{4}$$

Equation (1) represents the basic similarity variable for modeling tornadolike vortices. Equation (2) represents the swirl ratio defined for the tornado simulator, and (3) represents the form most readily determined through laboratory measurement. Equation (4) is in a form easier to interpret physically and represents the tangent of a characteristic helix angle of the flow through the updraft hole.

In the Purdue simulator, the four critical quantities, depth of inflow, radius of updraft hole, volume flow rate, and far-field tangential velocity, are each variable over a wide range of values. Estimates based on work accomplished to date indicate that the simulator can generate and maintain vortices for swirl ratios ranging from $\sim 10^{-2}$ up to ~ 30. Based on the results of previous investigations and present work, it appears that the swirl ratios of most interest in the laboratory (for vortex breakdown) lie in the range of $\sim 10^{-1}$ up to ~ 1.

Previous experimenters in this area have been limited in their work by the wandering of the vortex. This results, in large part, from turbulent components generated in the laboratory and drawn into the experimental volume. This problem has been removed by surrounding the inflow region with antiturbulence panels, and now highly stable vortex configurations can be established for a wide range of settings. Radius of vortex wander is now typically $<5\%$ of the radius of maximum winds, which makes it possible to obtain some flow measurements inside the core. Another stability feature adapted was to minimize surging in the extraction system by using a heavy fan wheel, a bypass duct system to allow the fan to see a constant load, and flow straighteners in the exhaust system.

The screen is carried on a two-ring assembly that consists of an upper load bearing ring and a lower drive ring, separated by spreader bars. The screen is stretched between the rings and is thus not part of the load bearing structure. The whole assembly is supported by castors with Timken bearings and is driven at the lower rim from a variable speed dc motor. Frictional forces have been minimized. This combination provides a screen rotation rate that is continuously variable over the range 0–11 rpm and is highly stable and vibration free at any speed. The ring assembly, which weighs 500 kg, has sufficient inertia to act as a flywheel in stabilizing the ring speed.

The key points made by Ward (1972) for formulating a valid vortex model of the tornado have been incorporated in the design. First, one must recognize that the tornado vortex forms through convergence processes restricted to a shallow layer near the surface. In the Purdue apparatus, this requirement is met by the convergence region in the lower one-quarter of the assemblage. The vorticity input from the screen to drive

[1] The definition of swirl ratio S given in (1) is consistent with the concept expressed by Davies-Jones (1973), which includes a factor of 2 in the denominator that is not contained in Lewellen's (1962) definition.

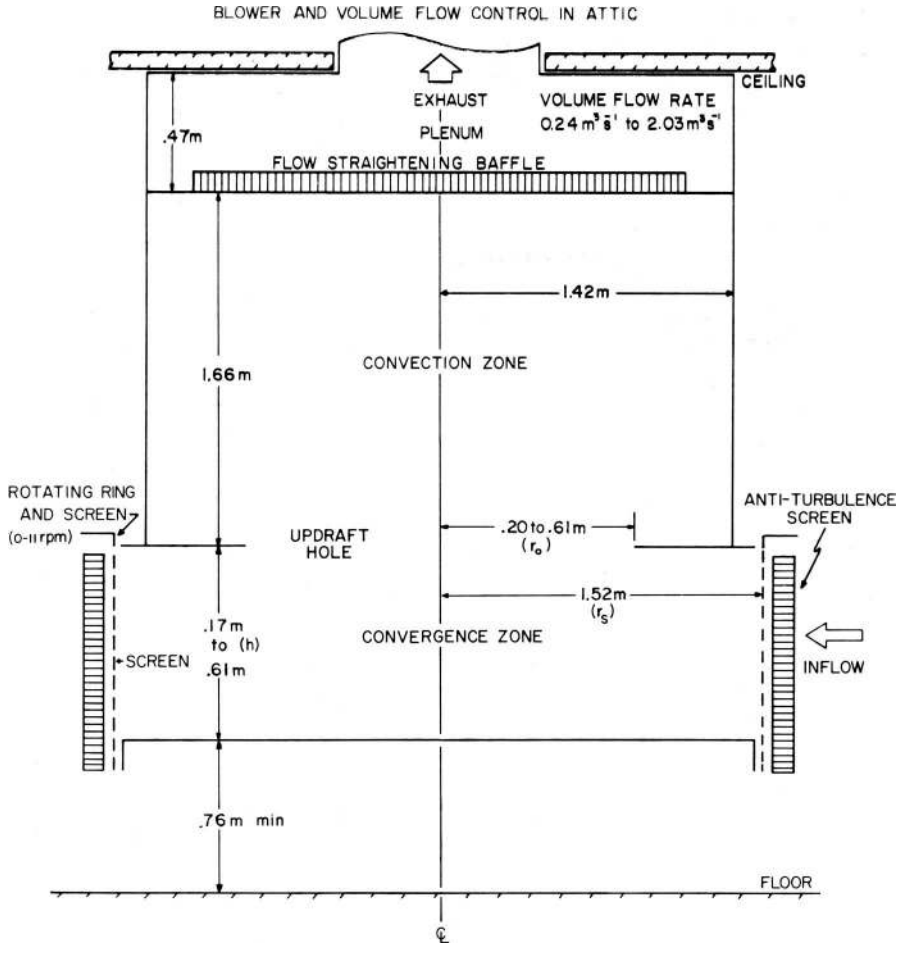

FIG. 3. Vertical cross-section schematic of the Purdue vortex simulator. The height and radius of the lower rotating chamber are defined as h and r_s. The circular opening at the top of the lower chamber has a radius of r_0.

the vortex enters from the bottom, which is in parallel with the natural process.

Second, the tornado must in some way be coupled to overlying straight-line horizontal flow wherein the horizontal pressure field is relatively uniform. This is accomplished in the experimental chamber by coupling the vortex to the suction source through a flow straightening baffle. This baffle ideally removes all rotation from the flow but allows unhindered axial flow. This insures that fan-induced vorticity does not affect the vortex. The use of a large plenum provides a uniform pressure over the top surface. Further, the baffle provides a relatively free upper boundary condition for the vortex. Such features as the radius of the ring of maximum air speed are then determined by the internal balance of forces within the vortex, and not by details of the exhaust orifice. This feature of the apparatus is essential to guarantee dynamic similarity in the core of the generated flow.

The major features of the completed Purdue vortex generator are also shown in Fig. 3.

3. Instrumentation and system evaluation

For qualitative observations of the flow, a visualization scheme using a "smoke" generator (actually a kerosene/light-oil boiler/recondenser) following an early design by Preston and Sweeting (1943) has been developed. When the kerosene/light-oil fog produced by this unit is introduced into the convergence region through injection holes in the lower surface, and back lighted at 135° with respect to the viewer, a brilliant white plume is observed. Banks of incandescent flood lamps in the upper chamber and a high-intensity spotlight in the convergence chamber provide illumination for viewing. Arrays of slaved electronic flash units in both chambers provide high-intensity bursts of light for photographic purposes.

A digital tachometer monitors the ring rotation rate by counting pulses generated by a light beam transmitted through each of 872 holes located at the circumference of the ring. Volume flow rate is obtained from a differential pressure probe placed in the exhaust duct connected to an appropriate transducer and signal con-

ditioning equipment. Air velocity measurements within the vortices are made with hot-film anemometry equipment consisting of a commercial system that has been modified and supplemented to meet the specific experimental requirements. Present efforts are concentrating on single-film hot-film measurements to determine the features of the main flow. This limits one to determining only the magnitude of the velocity vector and the yaw angle it makes with respect to a radial-axial plane. It is planned to begin using a split-film assembly in the near future. This will allow resolution of the pitch angle and thus permit determination of the velocity components.

A rigorous and extended evaluation of the performance of the simulator was undertaken to investigate and optimize the character of the flow and to assess the accuracy with which the swirl ratio S could be determined. The error in determining the volume flow rate was found to depend on the actual flow rate. The error is greater at lower flow rates and is typically 2% for the most commonly used range of flow rates. Fluctuations in the flow, which were linked to external sources, were virtually eliminated after taking appropriate measures. In related problems, it was found that the measured volumetric flow in the exhaust duct did not equal the flow rate through the eruption hole, implying some leakage. Some leakproofing was accomplished, after which a second test showed that the measured flow rate was equal to the flow through the duct to within experimental error (2%). At the same time, it was discovered that a significant amount of air entered the chamber not through the screen but by coming in around the ring. It was found that initially only about half of the air in the chamber came through the screen, and air entering by other paths interacted with it, creating a turbulent flow. This effect was eliminated by appropriate placement of air blocks.

The sharp lip around the updraft hole exerts a definite influence on the flow in the immediate vicinity of the edge, but this influence does not appear to alter significantly the flow in the regions of most interest. A need has been identified for shaping the updraft hole and providing a region of negative flare below the hole region. Also, since air rushing through the hole tends to form a circulation cell in the upper chamber (an undesirable feature), there is a requirement for a section with positive flare above the hole. The modification envisioned resembles a large Venturi tube. Investigation of the optimum shape is continuing.

Accuracy of the flow measurements made with the hot-film equipment was determined using a separate low-speed calibration wind tunnel. The absolute error in the magnitude of the flow vector over the range of 0.5–5 m s^{-1} is ± 0.05 m s^{-1}, relative errors being somewhat smaller. The error in the determination of yaw angle is $\pm 2°$. A related question is the length of filtering time required to obtain a representative value of the magnitude of the velocity at a point. This varies widely depending on location within the flow. Typical values are 25 s (5 s filter time constant) in far-field regions, to at least 50 s (10 s filter time constant) in the more turbulent regions. Measurements within the core may take several minutes due to the extremely high turbulence levels found in this region.

The error present in estimates of the swirl ratio S depends on the combined errors from the various quantities in (3). The error in the aspect ratio a depends only on the linear dimensions of the apparatus. These are easily measured with a high degree of accuracy, so that the uncertainty in the value of a is well under 1%. The numerator of (3) is the tangent of the yaw angle of the flow just inside the screen. As indicated above, present measurement and computational procedures provide values of yaw angle to within $\pm 2°$, and of its tangent to within $\pm 7\%$ (for a typical angle of 45°). This essentially represents the error in S.

4. Experimental results

Experimental work undertaken to date has had the following objectives:

1) determining qualitatively the range of vortex configurations that it is possible to generate with the apparatus;
2) evaluating the performance of the flow visualization scheme for making visible the complex three-dimensional swirling flow;
3) initial mapping of flows within the chamber using the single-film hot-film anemometer (under a variety of boundary conditions).[2]

a. Vortex configurations

It has been found that the unit is capable of generating a wide variety of swirling flows. The most interesting observations to date concern the sequence of events that appears to lead to vortex breakdown and the formation of the multiple vortex configuration.

It is observed that as the swirl ratio is increased from the zero (no swirl) state (so that circulation/vorticity is transported inward to form the vortex), a smooth, laminar-appearing vortex core region develops in the convergence region (Fig. 4a). This smooth core responds to small increases in swirl ratio by a radial contraction. However, investigation of the axial structure of the core shows that the core flow undergoes significant internal structural changes as the flow approaches the top baffle. The region characterized by this difference in structure moves upstream (i.e., downward) with increases in swirl ratio. It appears that in this region the maximum of vertical velocity moves off the central axis to form a cylindrical ring at the outer edge of the core zone. The vertical flow at the center line becomes relatively stagnant and shows a tendency to develop axial backflow, drawing air downward through the upper baffle. (This illustrates the importance of the upper baffle intro-

[2] This effort has been undertaken both to collect quantitative data on selected vortex configurations and to provide a more detailed evaluation of the performance of the vortex generator.

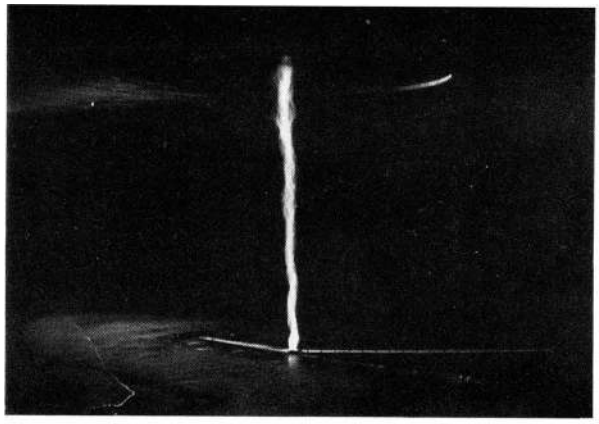

a. Single laminar funnel obtained under conditions of weak swirl.

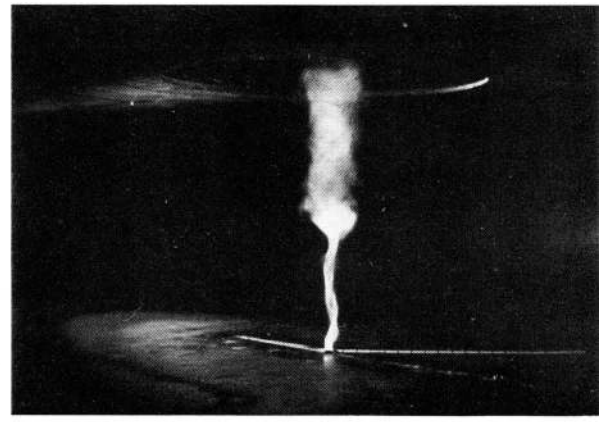

b. Free stagnation point separating upper turbulent core from the lower laminar vortex core.

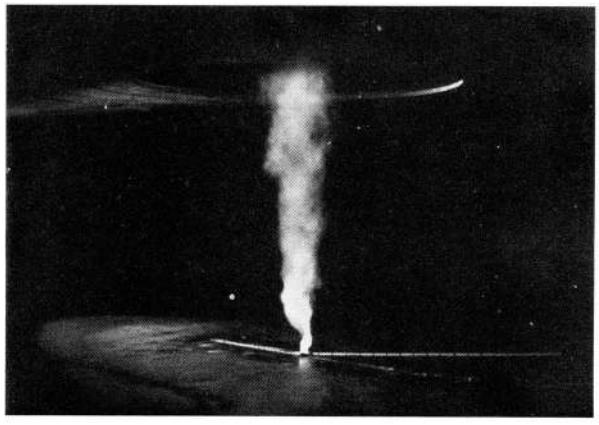

c. Turbulent core that results when the stagnation point moves all the way down to the bottom of the chamber.

d. Turbulent core that has undergone radial expansion as a result of further increase in the swirl ratio.

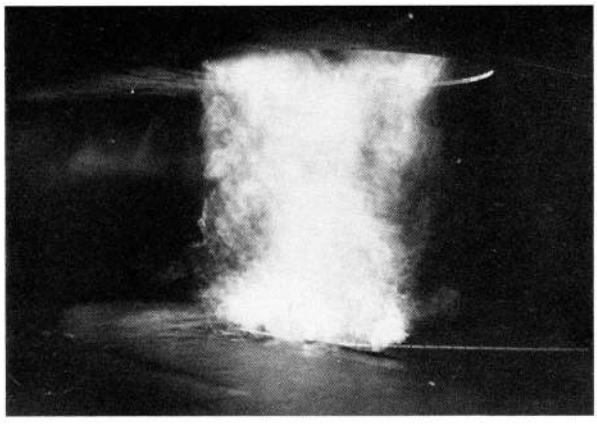

e. Two intertwined helical vortices, representative of a transitional stage between vortex breakdown and the formation of multiple subsidiary vortices in the convergence region.

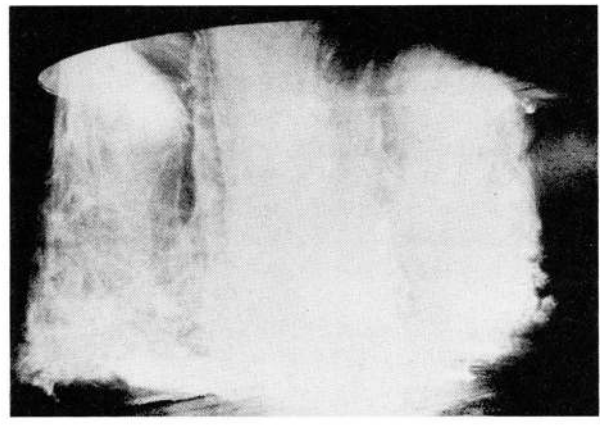

f. Configuration of four vortices.

FIG. 4(a–f). Vortex configurations simulated by the Purdue vortex generator, for conditions of increasing swirl ratio.

duced by Ward (1972) in his original apparatus.) Not only does this baffle eliminate the possibility of fan-induced vorticity influencing the vortex, but it also provides a relatively free exhaust (downstream) boundary condition so that the core radius is determined by the balance of forces within the core and by the geometry of the convergence and convection regions. Use of this baffle as the exhaust, with a large plenum above, frees the vortex from restrictions caused by the configuration of the exhaust orifice.

The breakdown in the core is characterized as a free stagnation point, in the form of a well-defined bubble (Fig. 4b) at the point where the downstream disturbance meets the rising upflow. The vortex core, downstream of the free stagnation point, has the structure of a relatively stagnant central region (with perhaps some downward motion), surrounded by a highly turbulent cylindrical layer. Such a configuration is highly likely to be unstable.

With further increases in the swirl ratio, two apparently interrelated events take place. First, the free stagnation point moves upstream until the lower surface is approached. The observer sees this approach as the descent of a "jump" or core expansion region to the surface, since the flow downstream of the "bubble" is significantly greater in radius when compared to the upstream core flow. Once the free stagnation point has descended to surface, the vortex presents the appearance of a boiling cylindrical column (Fig. 4c). Further increases in swirl ratio result in a general radial expansion of the core (Fig. 4d).

Second, during the descent of the bubble, increases in swirl appear to intensify or "thin" the cylindrical shear zone downstream of the free stagnation point to where the initial, single, quasi-cylindrical shear zone is no longer stable and the lowest-order disturbance mode is excited. This initial mode takes the form of first a single spiraling (helical) vortex and then interlocking helical spiral vortices (Fig. 4e). These events are observed as a "breakdown" and reorganization of the core zone into a new equilibrium configuration.

When the initiation of the disturbance takes place after the free stagnation point has reached surface, the rolling spiral vortices extend well down into the convergence region. This is apparently analogous to what occurs in a real tornadic event that gives rise to the "suction vortex phenomenon."

The Xenia, Ohio, tornado of 3 April 1974 is a good example of such an event, as two interlocking helical condensation funnels were photographed (Fujita, 1976) as well as suction debris vortices. When the magnitude of the swirl ratio is sufficiently large ($\sim$1), the disturbance vortices extend to the lower surface and exhibit a tendency to stand erect through the convergence region, tilting into a more helical pattern in the convection zone.

When the swirl ratio is increased still further, the equilibrium state progressively shifts to higher-order disturbances. Figure 4f shows a pattern of four vortices, with as many as seven subsidiary vortices having been observed embedded within the shear zone of the basic flow. In each case, it appears that the final form taken by the flow (visualized as consisting of the converging external flow, the stagnant core zone with surrounding shear layer, and the subsidiary vortices embedded within the shear layer) appears to be one in which the structure of the shear layer has been so modified by the presence of the disturbance vortices that a balance of forces again prevails within the core.

b. Quantitative velocity measurements

Measurements have been made of the flow velocity in the convergence region and, to a more limited extent, in the convection region immediately above the updraft hole. This work has been undertaken using a single-film hot-film probe, so that at present only the magnitude of the total mean velocity vector and the yaw angle of this vector in the horizontal plane with respect to the radial direction have been obtained. This activity is providing a quantitative data base concerning the flow within the chamber.

It has been found that the flow in much of the convergence region is quite smooth, so that data can be collected relatively rapidly with a minimum of filtering. This is not the case with the flow near the core. Here the flow appears to be highly turbulent. As a result, data collection is slow due to the filtering required to resolve a representative value of the mean velocity. The vortex flow field as a whole has been found to be relatively steady and to remain fixed in one position, with only a small meander about the mean position. It is anticipated that this small meander can be reduced even further once the details of the flow within the apparatus are fully appreciated.

It has also been determined that so long as the dimensions of the core radius are an order of magnitude or more larger than the cross-sectional radius of the probe stem, the presence of the probe has little or no readily observable effect on the core. An exception is found when the bubble is approached. This feature appears sensitive to local obstructions and shows a tendency to move up or downstream and "seize onto" a probe stem, a smoke inlet tube, etc., when such an object is moved nearby.

Areas of primary interest and concern in the collection of quantitative data are:

1) the edge effects due to the presence of the sharp lip at the orifice between the convergence and the convection regions;[3]
2) the shear zone downstream of the location of the free stagnation point;

[3] Findings thus far show that the vertical profile of the radial velocity (under both swirl and no-swirl conditions) is not symmetrical with respect to the horizontal midplane of the convergence region. Rather, a jet effect is present in the top half of the convergence region, which extends around the lip.

3) the corner region where the radial inflow in the lower one-half of the convergence region turns upward.

A cross-sectional plot of velocity magnitude and yaw angle for a vortex similar to that shown in Fig. 4e is displayed in Fig. 5. The velocity measurements were generally not extended into the core for $r < 5$ cm because of the large changes (compared to total signal output) in the values encountered in this region due to high turbulence levels and meanderings of the vortex axis. Also, the present anemometer calibration setup will only allow calibrations of the probes for the range 0.5–5 m s^{-1}, which therefore fall within this range.

Figure 6 is a plot for the vortex in Fig. 4e of $|\mathbf{V}|$ vs. r on log-log paper for $z = 7.5$ cm, for the boundary conditions noted. The idealized profile for a potential vortex with radial sink flow and solid body rotation is shown for convenience. Figure 6 shows the strong tendency for the flow to approximate the idealized Rankine flow model ($|\mathbf{V}| \propto r^{-1}$) in the lower one-half of the convergence region. Measurements have indicated, however, that near the top of the convergence region, the presence of the sharp orifice edge causes substantial departures from the idealized flow. However, although results show that the effect of the orifice is felt over a wide area within the flow, its effects appear to be minimal near the lower surface and in the core region (for this combination of depth and hole size). It is expected that implementation of the modification to the updraft hole will provide a more uniform transition between the convergence and the convective regions.

We can also note in Fig. 5 the tendency for the core to depart from a strict $|\mathbf{V}| \propto r^{-1}$ dependency and to develop a more complicated structure, for $z > 30$ cm. It is in this region that we find the beginning of the spiraling, helical pattern. Note also the complicated structure in the vicinity of $z = 7.5$ cm. Examination of this cross section and the photographic data indicates that the free stagnation point is most likely located at about $z = 10$ cm. The data suggest that what is shown for $7.5 \text{ cm} > z > 0$ cm is the turning aside around the free stagnation point of the jetlike flow resulting from the eruption of the surface boundary layer at the axis. The region near the axis has not yet been completely probed owing to the high turbulence levels and increasing larger-scale fluctuations due to the vortex wander encountered as the axis is approached.

5. Summary

The development of a tornado vortex simulator at Purdue University has been discussed and information presented that compares this system with the earlier machine modeled by Ward (1972). Selected photographs of vortex configurations obtained in the simulator have been presented that demonstrate the ability of the machine to achieve vortex breakdown and multiple vortex formation. A radial-axial profile of velocity magnitudes has been presented for the state of vortex break-

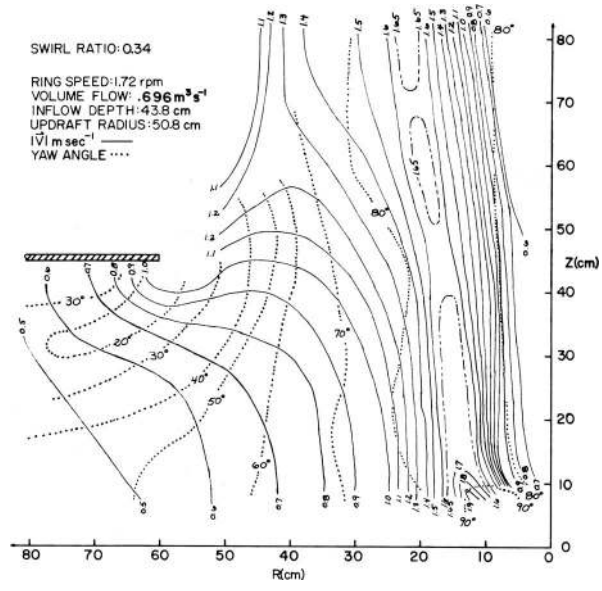

FIG. 5. Radial-axial presentation of mean flow field obtained with single-film sensor showing velocity magnitude contours (in meters per second) and yaw angle (with respect to the radial-axial plane) for a vortex characterized by a swirl ratio of 0.34.

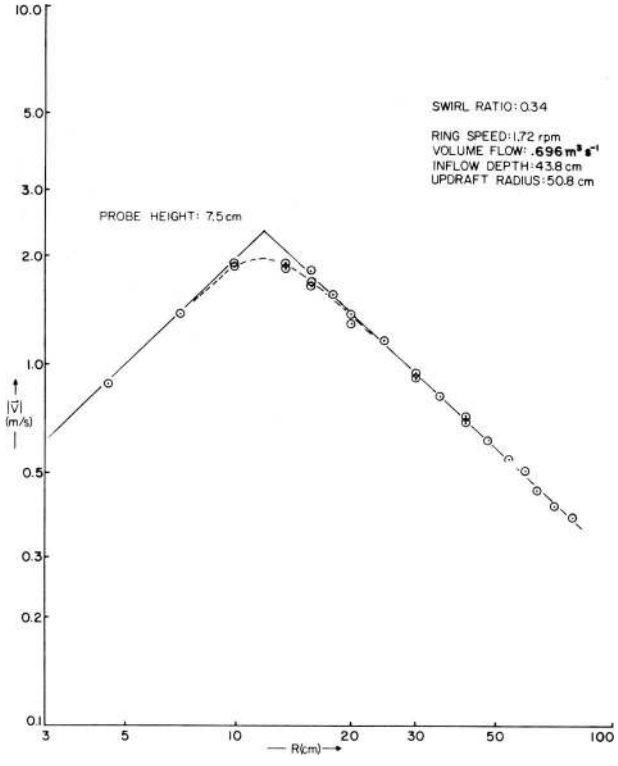

FIG. 6. Plot of log $|\mathbf{V}|$ vs. log R for a constant probe height of 7.5 cm. For comparison, the slopes corresponding to an idealized Rankine combined vortex of core radius 10 cm are shown.

down characterized by two interlocking helical spiral vortices. This preliminary result shows the potential that the experimental system offers in obtaining detailed information about the flow fields for various transitional stages of vortex appearance and formation. The flow field presented also demonstrates how possible effects introduced by the design of the apparatus can be detected and corrected (e.g., the sharp orifice edge of the updraft opening), thus yielding a more idealized flow.

The occurrence and significance of the multiple vortex phenomenon on different scales in the thunderstorm-tornado system have been brought to light in recent observational studies. Laboratory simulation allows one through a similarity approach to apply experimental findings to any scale of multiple vortex event in the atmosphere. In fact, the laboratory experimentation should yield a universal stability diagram that specifies the conditions for vortex breakdown and transition to multiple vortex patterns as a function of increasing swirl ratio. The unlikelihood of obtaining sufficient data to describe the flow field in the real tornado cyclone–tornado event makes the similarity approach an attractive one for investigating natural vortices. Laboratory study may also provide information that allows one to more properly interpret and understand the flow field in the surface boundary layer associated with the multiple suction vortex system in nature.

Efforts will continue to improve the design and operation of the vortex simulator and to photographically document the significant flow features for a wide range of swirl ratios. An effort is also being planned to determine the three-dimensional flow field by the use of split-film hot-film anemometry.

Acknowledgments. The authors would like to thank Mr. Glenn Baker for technical assistance and Ms. Gene Shelley for typing the manuscript. This research is supported by the National Science Foundation under the auspices of research grants ATM-75-15526 and ATM-76-00211.

References

Agee, E. M., C. R. Church, C. Morris, and J. T. Snow, 1975: Some synoptic aspects and dynamic features of vortices associated with the tornado outbreak of 3 April 1974. *Mon. Wea. Rev.*, **103**, 318–333.

——, J. T. Snow, and P. R. Clare, 1976: Multiple vortex features in the tornado cyclone and the occurrence of tornado families. *Mon. Wea. Rev.*, **104**, 552–563.

——, ——, F. S. Nickerson, P. R. Clare, C. R. Church, and L. A. Schaal, 1977: An observational study of the West Lafayette, Indiana, tornado of 20 March 1976. *Mon. Wea. Rev.*, **105**, 893–907.

Davies-Jones, R. P., 1973: The dependence of core radius on swirl ratio in a tornado simulator. *J. Atmos. Sci.*, **30**, 1427–1430.

——, 1976: Laboratory simulations of tornadoes. *Proceedings of a Symposium on Tornadoes: Assessment of Knowledge and Implications for Man,* Texas Tech Univ., Lubbock, Tex., 151–174.

Fujita, T. T., 1959: Detailed analysis of the Fargo tornadoes of 20 June 1957. SMRP Tech. Rep. 5, Univ. of Chicago, Chicago, Ill., 29 pp.

——, 1971: Proposed mechanism of suction spots accompanied by tornadoes. *Preprints, Seventh Conference on Severe Local Storms (Kansas City),* AMS, Boston, pp. 208–213.

——, 1976: Graphic examples of tornadoes. *Bull. Amer. Meteor. Soc.*, **57**, 401–412.

Georges, T. M., 1976: Infrasound from convective storms—Part 2: A critique of source candidates. NOAA Tech. Rep., ERL 380-WPL 49, U.S. Dept. of Commerce, Washington, D.C., 59 pp.

Golden, J. H., and D. Purcell, 1975: Photogrammetric velocities for the Great Bend, Kansas, tornado—Accelerations and asymmetries. *Preprints, Ninth Conference on Severe Local Storms (Norman, Okla.),* AMS, Boston, pp. 336–343.

Hoecker, W. H., Jr., 1960: Wind speed and air flow patterns in the Dallas tornado of 2 April 1957. *Mon. Wea. Rev.*, **88**, 167–180.

Jischke, M. C., and M. Parang, 1974: Properties of simulated tornado-like vortices. *J. Atmos. Sci.*, **31**, 506–512.

——, and ——, 1975: Fluid dynamics of a tornado-like flow. Final report, grant N22-200-72(G), NSSL/NOAA, Norman, Okla.

Lewellen, W. S., 1962: A solution for three-dimensional vortex flows with strong circulation. *J. Fluid Mech.*, **14**, 420–432.

Preston, J. G., and N. E. Sweeting, 1943: An improved smoke generator for use in the visualization of airflow, particularly boundary layer flows at high Reynolds numbers. R&M 2023, ARC 7111, Aeronaut. Res. Counc., London, 8 pp.

Van Tassel, E. L., 1955: The North Platte Valley tornado outbreak of 27 June 1955. *Mon. Wea. Rev.*, **83**, 255–264.

Ward, N. B., 1972: The exploration of certain features of tornado dynamics using a laboratory model. *J. Atmos. Sci.*, **29**, 1194–1204.